

DTIC FILE COPY

4

RADC-TR-89-211
In-House Report
October 1989



AD-A219 305

PERFORMANCE OF ADAPTIVE NULLING ANTENNAS IN A JAMMING ENVIRONMENT

Lisa M. Sharpe

DTIC
ELECTE
MAR 20 1990
S B D

APPROVED FOR PUBLIC RELEASE; DISTRIBUTION UNLIMITED.

ROME AIR DEVELOPMENT CENTER
Air Force Systems Command
Griffiss Air Force Base, NY 13441-5700

90 03 20 128

This report has been reviewed by the RADC Public Affairs Office (PA) and is releasable to the National Technical Information Service (NTIS). At NTIS it will be releasable to the general public, including foreign nations.

RADC TR-89-211 has been reviewed and is approved for publication.

APPROVED:



ROBERT J. MAILLOUX, Chief
Antennas and Components Division
Directorate of Electromagnetics

APPROVED:



JOHN K. SCHINDLER
Director of Electromagnetics

FOR THE COMMANDER:



JOHN A. RITZ
Directorate of Plans and Programs

If your address has changed or if you wish to be removed from the RADC mailing list, or if the addressee is no longer employed by your organization, please notify RADC (EEAA) Hanscom AFB MA 01731-5000. This will assist us in maintaining a current mailing list.

Do not return copies of this report unless contractual obligations or notices on a specific document requires that it be returned.

REPORT DOCUMENTATION PAGE

Form Approved
OMB No. 0704-0188

1a. REPORT SECURITY CLASSIFICATION Unclassified			1b. RESTRICTIVE MARKINGS		
2a. SECURITY CLASSIFICATION AUTHORITY			3. DISTRIBUTION / AVAILABILITY OF REPORT Approved for public release; distribution unlimited.		
2b. DECLASSIFICATION / DOWNGRADING SCHEDULE			5. MONITORING ORGANIZATION REPORT NUMBER(S)		
4. PERFORMING ORGANIZATION REPORT NUMBER(S) RADC-TR-89-211			7a. NAME OF MONITORING ORGANIZATION		
6a. NAME OF PERFORMING ORGANIZATION Rome Air Development Center		6b. OFFICE SYMBOL (If applicable) EEAA	7b. ADDRESS (City, State, and ZIP Code)		
6c. ADDRESS (City, State, and ZIP Code) Hanscom AFB Massachusetts 01731-5000			9. PROCUREMENT INSTRUMENT IDENTIFICATION NUMBER		
8a. NAME OF FUNDING / SPONSORING ORGANIZATION Rome Air Development Center		8b. OFFICE SYMBOL (If applicable) EEAA	10. SOURCE OF FUNDING NUMBERS		
8c. ADDRESS (City, State, and ZIP Code) Hanscom AFB Massachusetts 01731-5000			PROGRAM ELEMENT NO. 62702F	PROJECT NO. 4600	TASK NO. 14
			WORK UNIT ACCESSION NO. 02		
11. TITLE (Include Security Classification) Performance of Adaptive Nulling Antennas in a Jamming Environment					
12. PERSONAL AUTHOR(S) Sharpe, L. M.					
13a. TYPE OF REPORT In House		13b. TIME COVERED FROM 9/88 TO 6/89		14. DATE OF REPORT (Year, Month, Day) 1989 October	
15. PAGE COUNT 22					
16. SUPPLEMENTARY NOTATION					
17. COSATI CODES			18. SUBJECT TERMS (Continue on reverse if necessary and identify by block number)		
FIELD	GROUP	SUB-GROUP	Adaptive Nulling, Visibility		
17	11				
17	06				
19. ABSTRACT (Continue on reverse if necessary and identify by block number) This report contains analysis of the performance of an adaptive nulling array in a jamming environment for various sizes of antenna arrays. Performance of adaptive nulling arrays and arrays with Chebychev tapering are compared.					
20. DISTRIBUTION/AVAILABILITY OF ABSTRACT <input type="checkbox"/> UNCLASSIFIED/UNLIMITED <input checked="" type="checkbox"/> SAME AS RPT. <input type="checkbox"/> DTIC USERS			21. ABSTRACT SECURITY CLASSIFICATION Unclassified		
22a. NAME OF RESPONSIBLE INDIVIDUAL Lisa M. Sharpe			22b. TELEPHONE (Include Area Code) (617) 377-4664		22c. OFFICE SYMBOL RADC/EEAA

Contents

1. INTRODUCTION	1
2. DISCUSSION	1
3. RESULTS	4
4. CONCLUSIONS	9
5. RECOMMENDATIONS	9
REFERENCE	17

Accession For	
NTIS GRA&I	<input checked="" type="checkbox"/>
DTIC TAB	<input type="checkbox"/>
Unannounced	<input type="checkbox"/>
Justification	
By	
Distribution/	
Availability Codes	
Dist	Avail and/or Special
A-1	

Illustrations

1. Adaptive Nulling Array Antenna System	2
2. Radiation Pattern for 50 Element Antenna with Jammers at $\pm 1.6^\circ$	5
3. Radiation Pattern for 50 Element Antenna with Jammers at $\pm 2.0^\circ$ and -1.2°	6
4. Interference Model	7
5. Visibility vs Antenna Size with Constant Power Antenna	8
6. Visibility vs Antenna Size Using T/R Modules	10
7. Probability of Detection vs Antenna Size With Constant Power Antenna	11
8. Probability of Detection vs Antenna Size Using T/R Modules	12
9. Adaptive Nulling Antenna and Chebychev Antenna Performance Comparison for Constant Power Antennas	13
10. Adaptive Nulling Antenna and Chebychev Antenna Performance Comparison Using T/R Modules	14

Performance of Adaptive Nulling Antennas in a Jamming Environment

1. INTRODUCTION

In a communications environment where there are many undesirable electromagnetic interferences that will degrade the capabilities of an antenna to receive a desired signal, adaptive nulling techniques can be used to minimize the effects of the undesirable signals while causing minimal loss to the desired signal. By using an adaptive nulling system, the spatial selectivity of an array antenna can be considerably increased.

The conventional low sidelobe antenna that is typically used in a noisy environment cannot perform as well as an adaptive antenna array because of the considerable beam broadening characteristic of a low sidelobe pattern. When the beam is made narrow, as in a uniformly illuminated array, the number of main beam interferences is reduced. The increased sidelobe level is a disadvantage, but sidelobe nulling has a minimal effect on the radiation pattern.

This report will show the expected performance of an adaptive nulling array using digital beamforming techniques as well as a comparison between an adaptive nulling antenna and a conventional low sidelobe antenna.

2. DISCUSSION

The adaptive nulling array antenna system is shown in Figure 1. The desired source, A, has magnitude a and direction θ . The interfering sources, B_k , have magnitude b_k , and direction θ_k^1 , where

(Received for publication 3 November 1989)

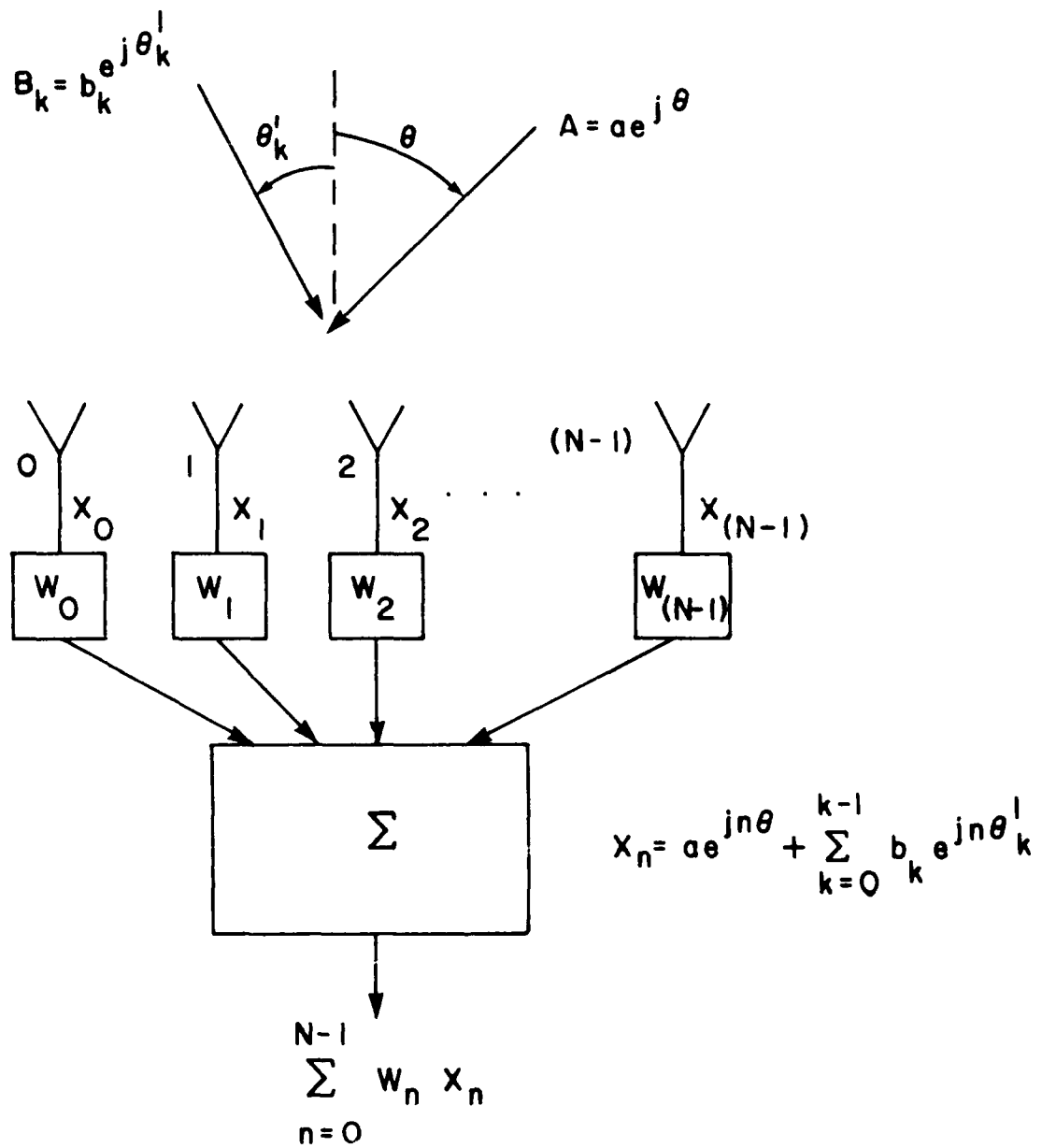


Figure 1. Adaptive Nulling Array Antenna System

k is the total number of interferences. The signal received at each antenna element, denoted by X_n , is the sum of the desired signal plus all the interfering signals. These received signals are then multiplied by the adapted weights calculated for each element. The signals from each element are then summed to achieve the radiation pattern of the array. The adaptive weights, w_n , are chosen so as to maximize the signal-to-interference-plus-noise ratio in the output of the antenna. This ratio can be written as:¹

$$\text{SINR} = \frac{P_s}{P_n} = |A|^2 \times \frac{w^t(ss^t)w}{w^tR_nw} \quad (1)$$

The vector s corresponds to the vector in the look direction, where the signal is known, while R_n , the noise plus interference covariance matrix, is unknown and must be measured in the absence of the desired signal. It can be shown that the weight vector w that maximizes SINR is:

$$w = \alpha R^{-1} s \quad (2)$$

where α is a constant of proportionality. Using the sample matrix inversion method, the weights can then be calculated directly from this equation.

These weights are the necessary coefficients used to place nulls in the directions of the interferences while maximizing the signal in the direction of the main beam. Although the signal in the direction of the main beam is maximized, gain loss will occur and can be considerable, depending on the position of the interferences and the size of the antenna.

An analysis has been performed to determine what effects antenna size has on the losses incurred when using adaptive cancellation techniques. This analysis was done for an ideal digital beamforming system. Also, the results presented are for a narrowband system. For a wideband system, the losses would be greater than those presented here.

The important parameter calculated was visibility over a specific angular sector and jammer density. This visibility was defined as the percent of the angular sector where the loss in the main beam did not fall below the specified loss. The ability to scan the main beam was used to achieve the maximum visibility.

Two different cases for power were considered. The first was for constant power, such as in a tube fed antenna, where the power does not change when the antenna size is changed. The second case corresponds to an antenna with T/R modules where the power increases linearly as the number of elements is increased.

The noise environment was modelled by an interference density. This density is defined as the number of jammers in a specific angular sector. The angular sector that contains one jammer is defined as β . Calculations of visibility were made over a 2β sector. The interference sources are able to move relative to the antenna. For example, if there are 10 interferences over a 32 degree sector, this would be an interference density of one jammer per 3.2° sector, so $\beta = 3.2^\circ$. The 2β sector over which the visibility would be calculated is 6.4° . By knowing β , the visibility can be determined for a specific antenna size, or conversely, the necessary antenna size for a desired visibility can be determined.

1. Steyskal, H. (1987) Digital beamforming antennas, an introduction, *Microwave Journal* 30,(No.1):107-124.

Figures 2 and 3 show some sample patterns for a 50 element antenna with $\beta = 3.2$ for two different jammer spacings.

The motion of the jammers was modelled as following a racetrack course. While one line of jammers is travelling in one direction, another line of jammers will be travelling in the opposite direction. In the model the 2β distance, the distance between two jammers travelling in one direction, will remain constant, while the other jammer, travelling in the opposite direction, will travel throughout the 2β sector. The visibility over the 2β sector will depend on the position of this third jammer. The interference model is shown in Figure 4.

3. RESULTS

Figure 5 shows the visibility curves as a function of jammer spacing and antenna size for the normalized power case. Because visibility is a function of jammer density as well as antenna size, the desired point on the abscissa is determined from both of these values. The four separate cases shown in Figure 4 are for various jammer positions. In the first case, the jammers are evenly spaced by a distance, 1β . In the second case, the central jammer has moved closer to one of the outer jammers than the other. The spacing is now $.75\beta$ between the central jammer and closer jammer, and 1.25β between the central jammer and the other jammer. The movement of the central jammer continues until, in case 4, the moving jammer is directly behind the outer jammer so that the two jammers are seen as one interference and the distance between two adjacent jammers as 2β . As would be expected, better visibilities are achieved with larger antennas in all cases. From these results, however, it is seen that there is not a simple linear relationship between size and performance. For the symmetric jammer spacing (1β) the performance will increase dramatically with antenna size up to approximately $\frac{\beta}{\lambda/U} = 80$. As the antenna size increases beyond this point, the performance begins to level off.

For widely spaced jammers, however, the performance shows a fairly small change as antenna size is increased. For example, to increase from $\frac{\beta}{\lambda/U} = 64$ to $\frac{\beta}{\lambda/U} = 96$, a 50 percent increase in antenna size, only a 5 - 10 percent increase in performance is realized.

The intermediate cases have curves that are not as smooth. This is because when the intermediate jammer is close to one of the outer jammers, there is no visibility between the closely spaced jammer until a fairly large antenna is used. When the antenna size is increased to the point where it is possible to see between closely spaced jammers, the performance will rapidly increase with antenna size.

This is evident in the case where the jammer spacing is 1.25β , 0.75β . In this case, the performance is fairly flat until visibility is achieved in both sections. The 7 dB curve, for instance, starts out rather flat, but when the size is increased beyond $\frac{\beta}{\lambda/U} = 80$, the visibility increases much more rapidly. The 1.5β , $.5\beta$ curves do not show this because for the antenna sizes shown, no visibility was achieved between the jammers that were separated by $.5\beta$. This is also the reason why the 1.5β , $.5\beta$ case gives the worst performance for the larger size antennas. Some visibility is seen between the 1.5β spaced jammers, even for the smaller antennas, but the visibility does not increase as rapidly with antenna size as the other cases because no visibility is achieved between the 0.5β spaced jammers.

The second case studied was the T/R module case. Because in this case the power increases with antenna size, the performance will improve more rapidly than in the previous case. This analysis was

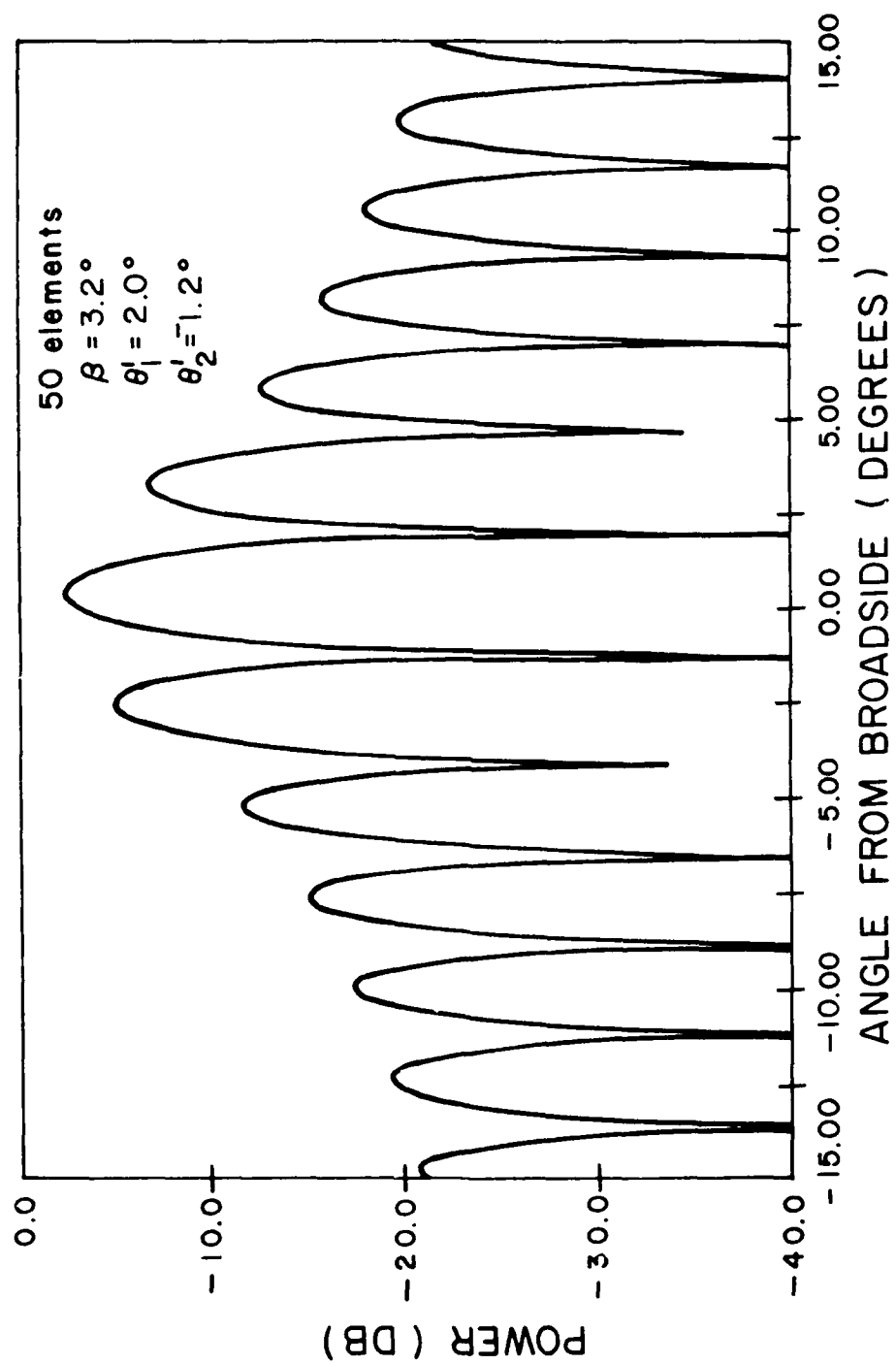


Figure 2. Radiation Pattern for 50 Element Antenna with Jammers at $\pm 1.6^\circ$

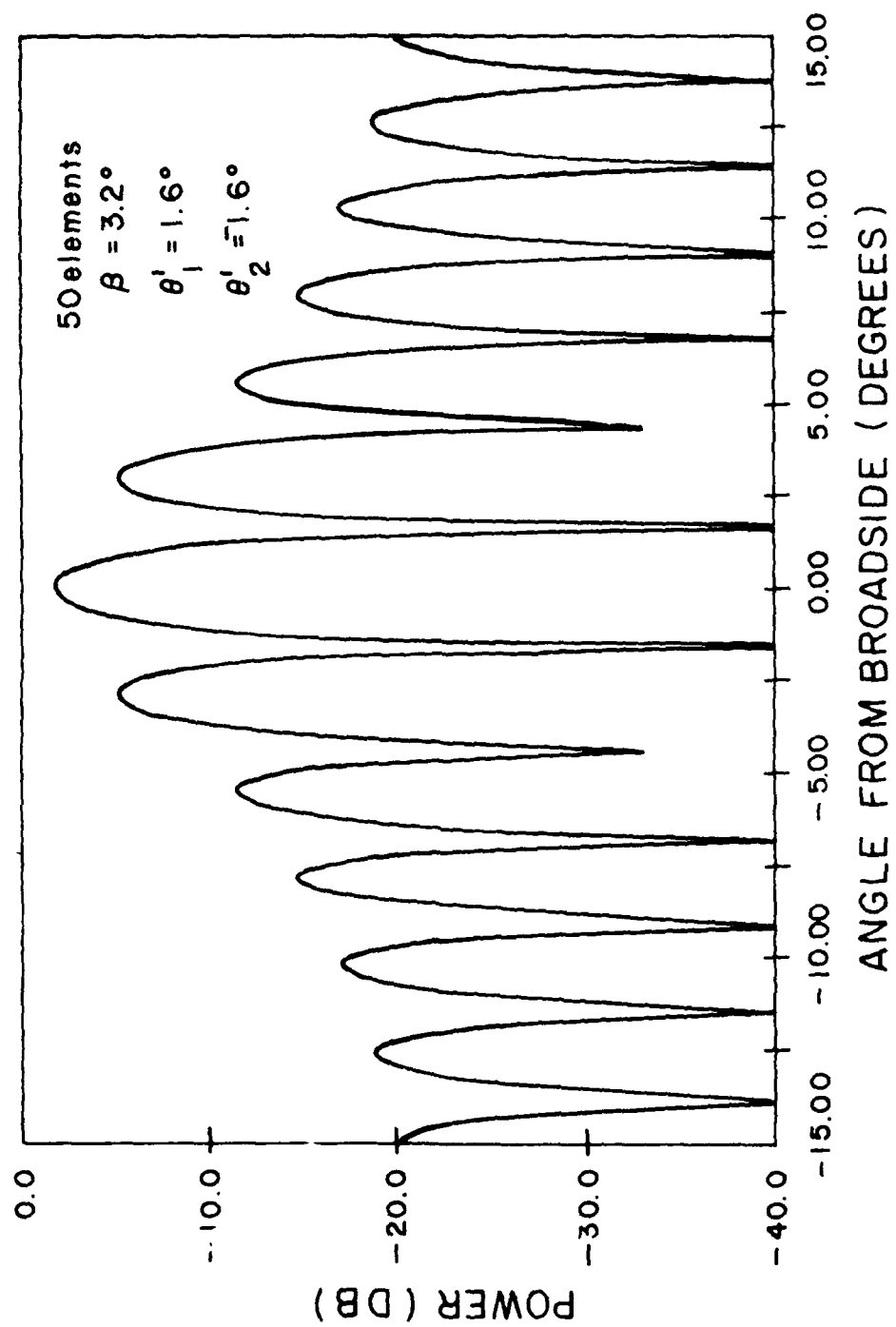


Figure 3. Radiation Pattern for 50 Element Antenna with Jammers at $\pm 2.0^\circ$ and -1.2°

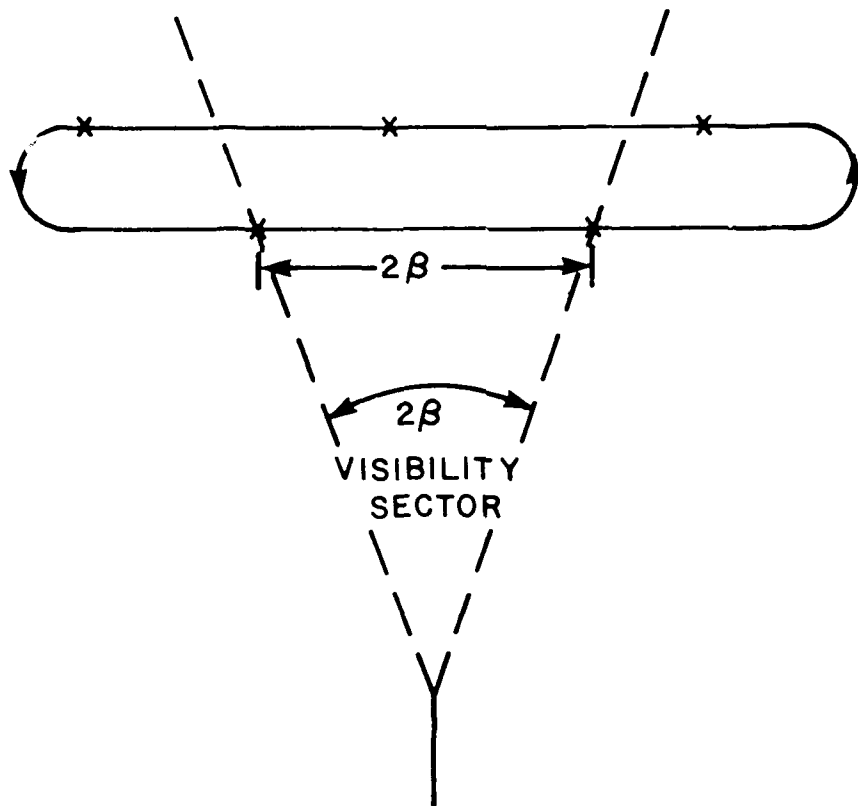


Figure 4. Interference Model

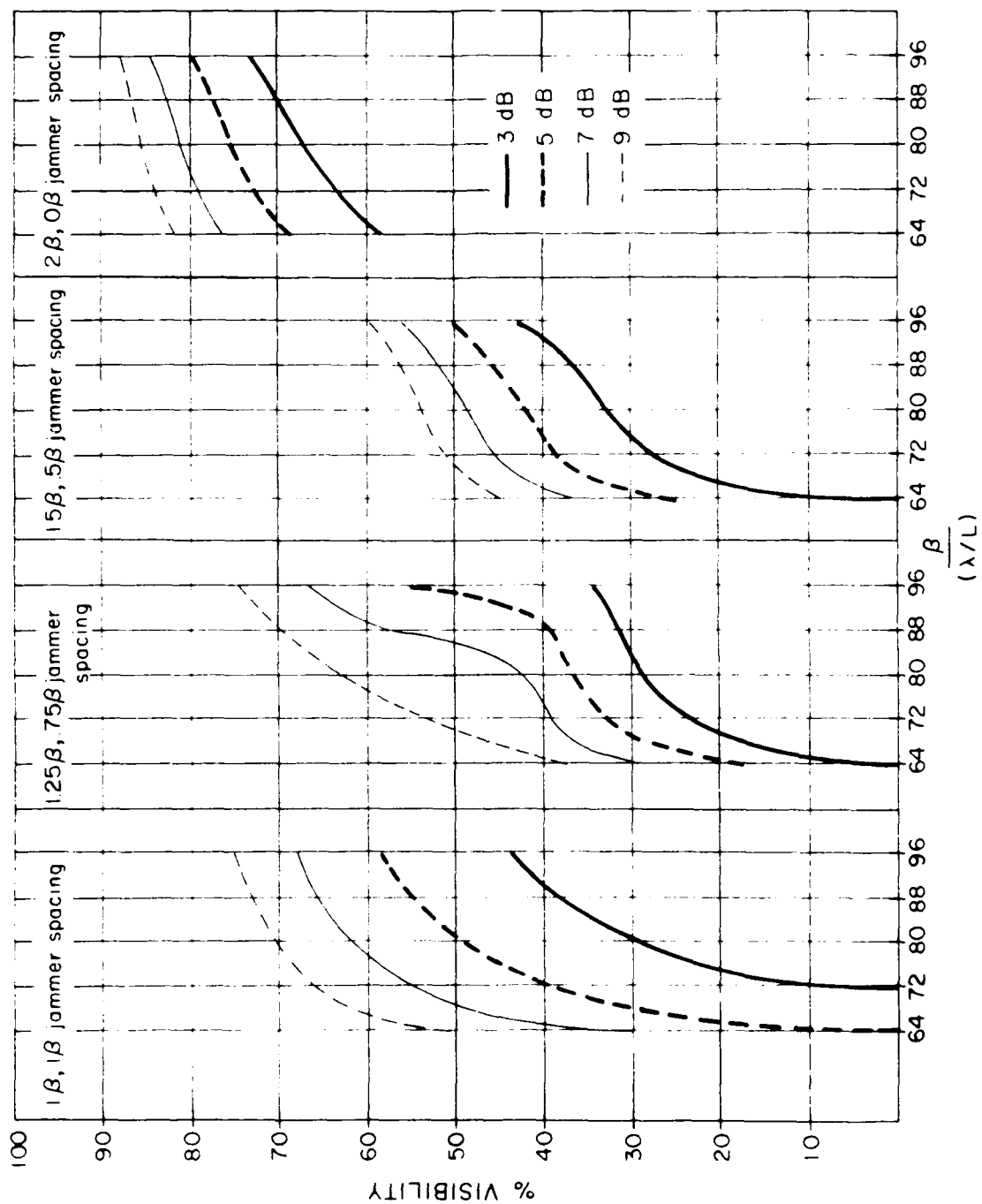


Figure 5. Visibility vs Antenna Size with Constant Power Antenna

done with the power normalized to the $\frac{\beta}{(\lambda/L)} = 64$ antenna size, so the $\frac{\beta}{(\lambda/L)} = 96$ antenna would have 1.5 times more power than the $\frac{\beta}{(\lambda/L)} = 64$ antenna.

Figure 6 shows the visibility curves for this case. As one would expect, the visibility is consistently higher than in the previous analysis. The difference in visibility is even more pronounced in the intermediate cases. This is because visibility occurs between the closely spaced jammers at smaller antenna sizes. Even in the $1.5\beta, 0.5\beta$ spacing, the $\frac{\beta}{(\lambda/L)} = 96$ size antenna just starts to gain some visibility between the closely spaced jammers with 9 dB of loss.

Figures 7 and 8 show the probability of detecting a target inside the 2β sector for the two different cases considered. This is calculated by averaging the visibilities for the jammer positions as the third jammer travels throughout the 2β sector. These figures clearly show that a large antenna is necessary to achieve an acceptable level of target detection.

A comparison was made between an adaptive nulling antenna and an antenna with low sidelobes to determine how much better performance could be expected using adaptive nulling techniques. For the low sidelobe antenna, the visibility was defined to be the portion of the 2β sector in which a SNR of 50 dB could be attained when the sidelobes were 50 dB, and a SNR of 60 dB when the sidelobes were 60 dB. The noise level was defined to be the level at which the jammer intersected the main beam.

Figures 9 and 10 show the comparisons for the constant power case and the T/R module case, respectively. From these figures it is clear that a considerably larger low sidelobe antenna must be used to achieve any visibility in a jamming environment. Once this critical size has been reached, however, the visibility improves rapidly with small increases in antenna size. However, in order for the low sidelobe antenna to achieve the same performance as the adaptive nulling antenna, much larger antennas would be required, and this may be unrealistic for UHF or lower frequency antennas.

4. CONCLUSIONS

The performance of adaptive nulling antennas is related to both the jamming environment in which they are operated and the size of the array used. Operation in a dense jamming environment requires a large antenna array to cancel the jammers while maintaining an acceptable amount of gain in the main beam.

A comparison between conventional low sidelobes antennas and adaptive nulling antennas shows that much better performance can be expected from the adaptive nulling antennas at considerably smaller antenna sizes.

5. RECOMMENDATIONS

The results presented in this report are for locating targets in a jamming environment. Once the targets have been located, it is necessary to track the target's motion. Monopulse is a common technique employed for target tracking. A future study will be performed to determine the performance of monopulse tracking in a jamming environment.

Because each element in a digital beamforming array requires its own digital beamforming hardware, the complexity of building large digital beamformers is a drawback. To achieve similar

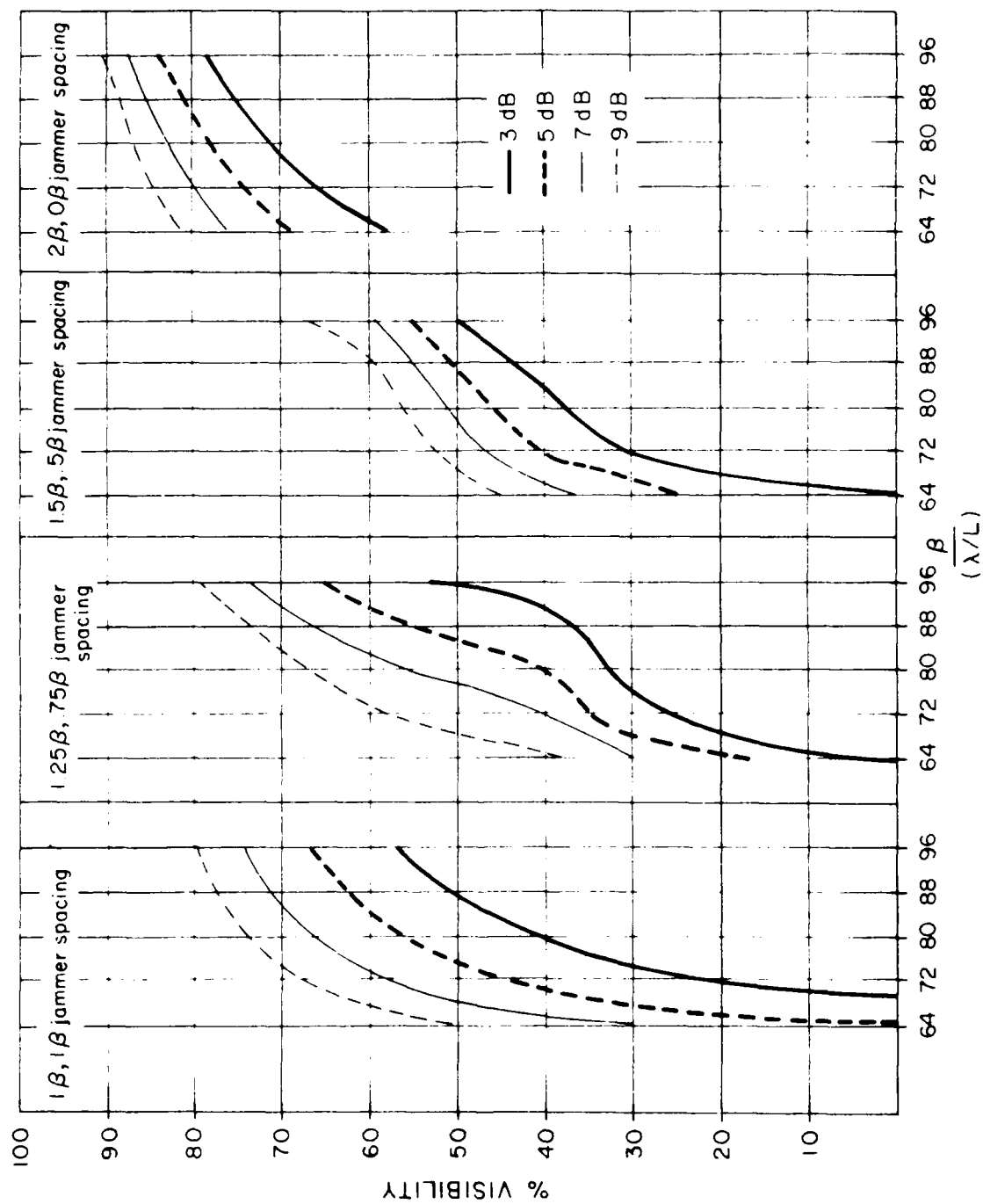


Figure 6. Visibility vs Antenna Size Using T/R Modules

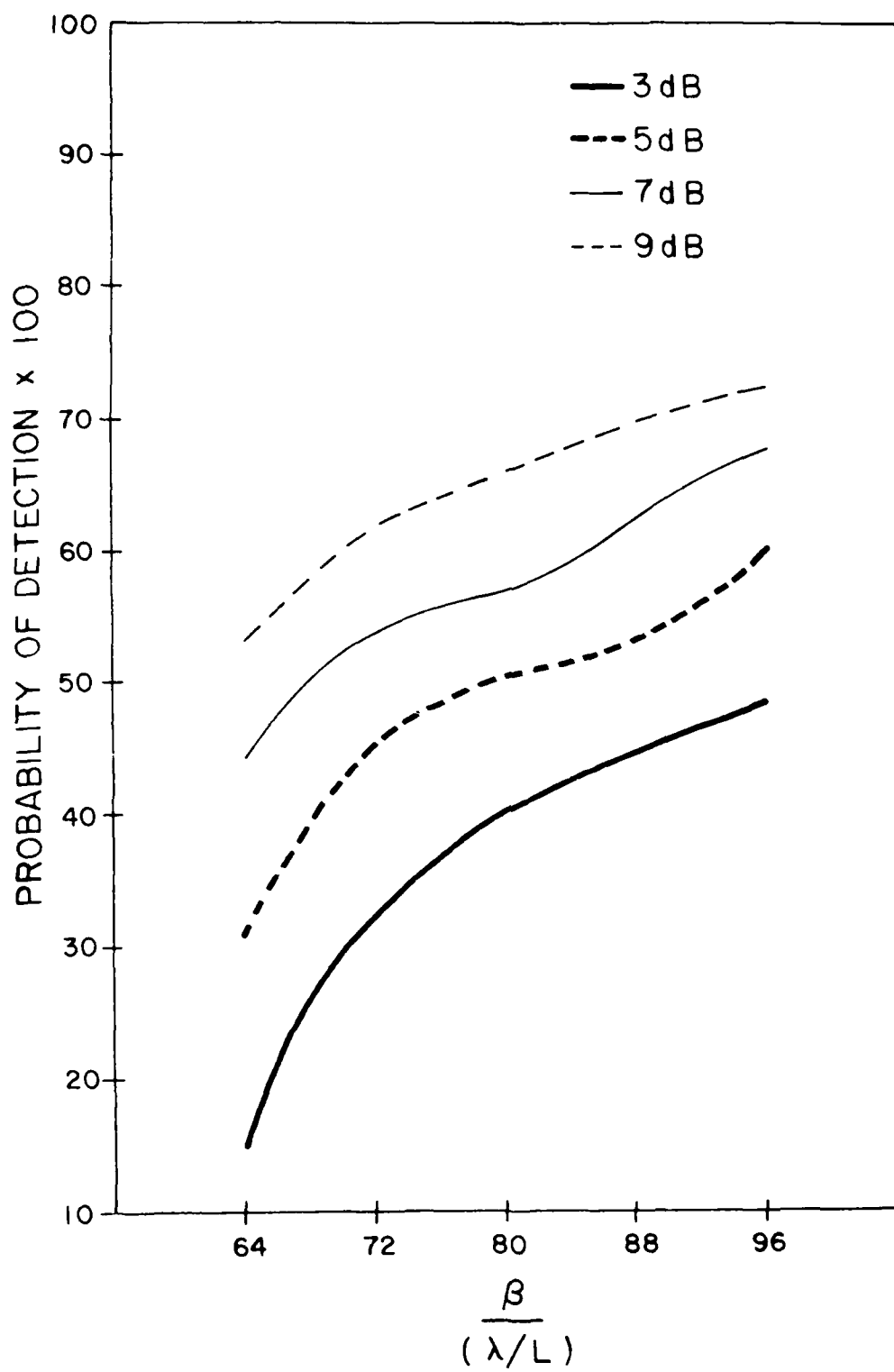


Figure 7. Probability of Detection vs Antenna Size with Constant Power Antenna

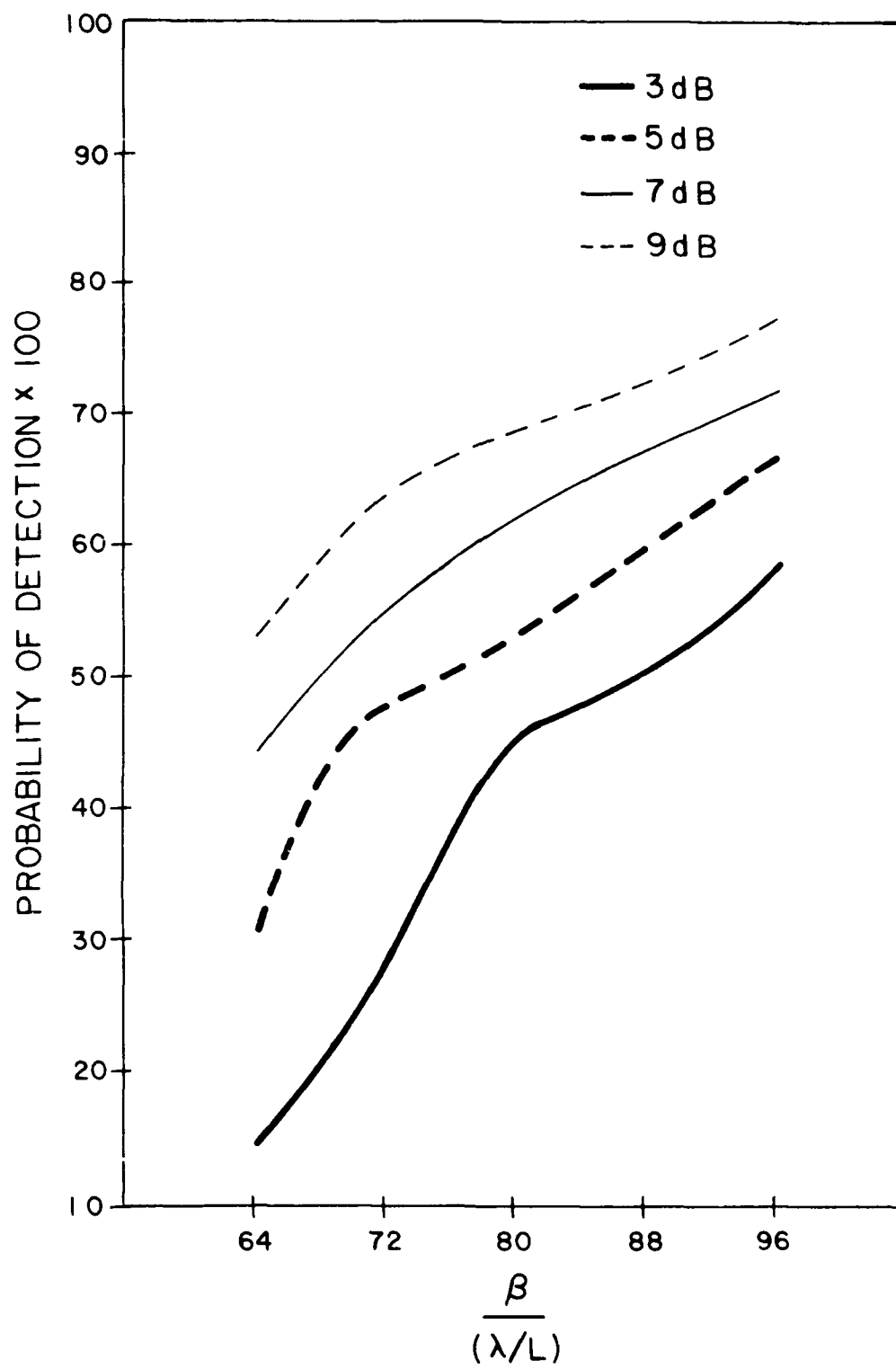


Figure 8. Probability of Detection vs Antenna Size Using T/R Modules

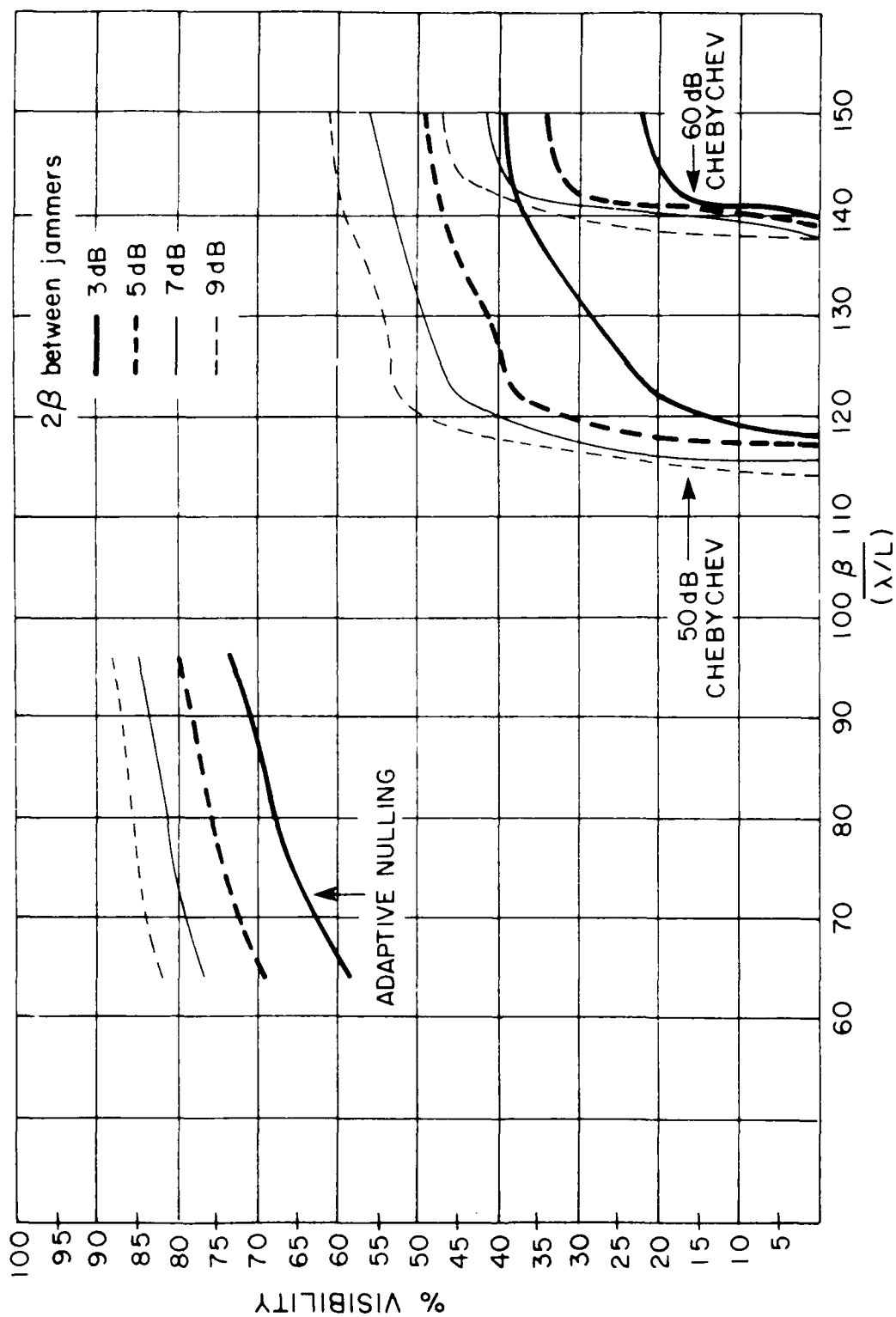


Figure 9. Adaptive Nulling Antenna and Chebyshev Antenna Performance Comparison for Constant Power Antennas

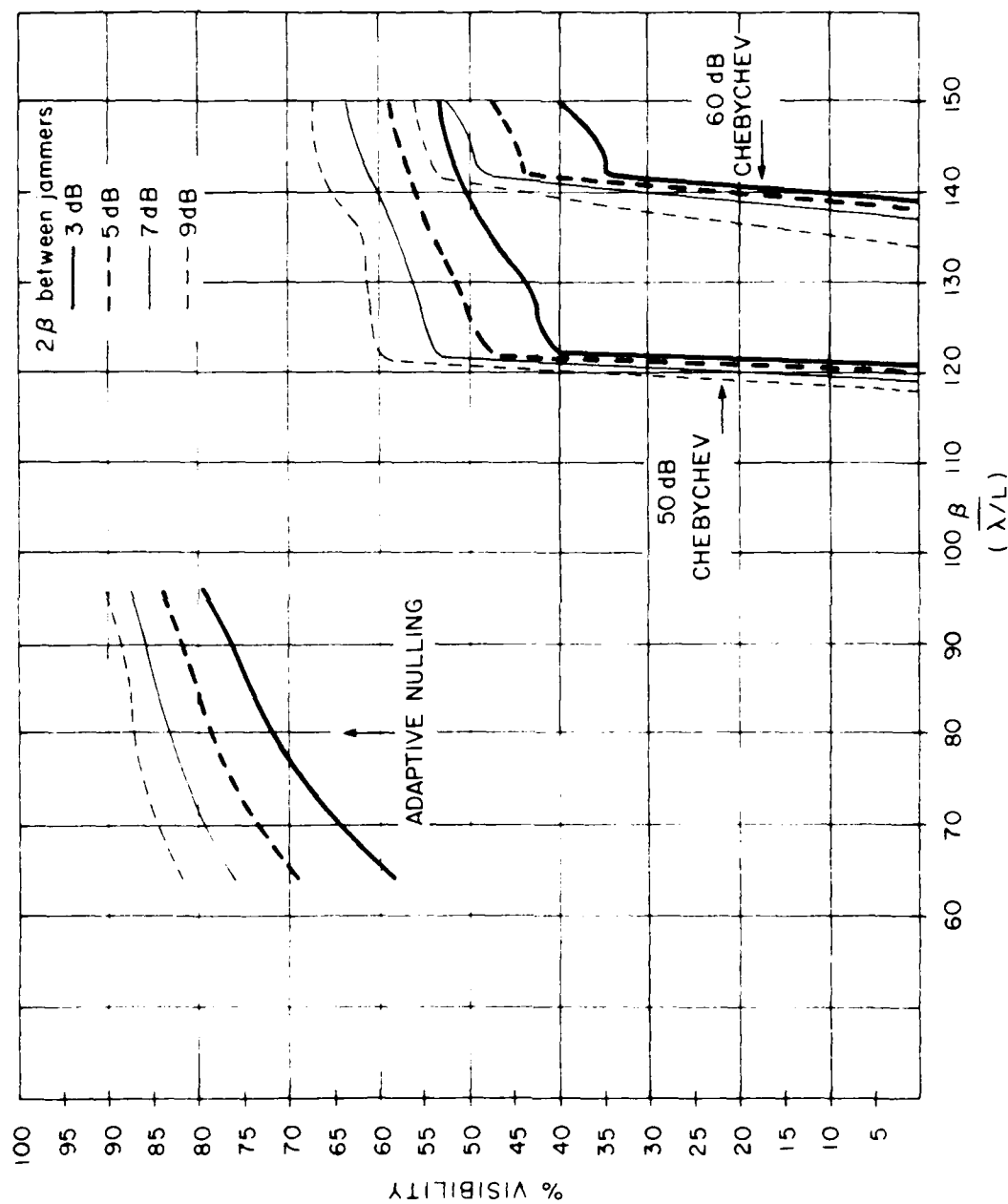


Figure 10. Adaptive Nulling Antenna and Chebyshev Antenna Performance Comparison Using T/R Modules

performance with less complexity, the array can be split into subarrays with each subarray having a separate digital beamforming network. A study should be performed to determine the level of performance one could expect from such a system.

Reference

1. Steyskal, H. (1987) Digital beamforming antennas, an introduction, *Microwave Journal* **30**,(No.1):107-124.



MISSION of Rome Air Development Center

RADC plans and executes research, development, test and selected acquisition programs in support of Command, Control, Communications and Intelligence (C³I) activities. Technical and engineering support within areas of competence is provided to ESD Program Offices (POs) and other ESD elements to perform effective acquisition of C³I systems. The areas of technical competence include communications, command and control, battle management information processing, surveillance sensors, intelligence data collection and handling, solid state sciences, electromagnetics, and propagation, and electronic reliability/maintainability and compatibility.